

# Self-formed bedrock waterfalls

Joel S. Scheingross<sup>1,2,3\*</sup>, Michael P. Lamb<sup>1</sup> & Brian M. Fuller<sup>1</sup>

**Waterfalls are inspiring landforms that set the pace of landscape evolution as a result of bedrock incision<sup>1–3</sup>. They communicate changes in sea level or tectonic uplift throughout landscapes<sup>2,4</sup> or stall river incision, disconnecting landscapes from downstream perturbations<sup>3,5</sup>. Here we use a flume experiment with constant water discharge and sediment feed to show that waterfalls can form from a planar, homogeneous bedrock bed in the absence of external perturbations. In our experiment, instabilities between flow hydraulics, sediment transport and bedrock erosion lead to undulating bedforms, which grow to become waterfalls. We propose that it is plausible that the origin of some waterfalls in natural systems can be attributed to this intrinsic formation process and we suggest that investigations to distinguish self-formed from externally forced waterfalls may help to improve the reconstruction of Earth history from landscapes.**

Waterfalls are thought to form when rivers cross lithologic boundaries<sup>2</sup>, or through an external (allogenic) perturbation to riverbed topography such as sea-level change<sup>2</sup>, fault displacement<sup>6,7</sup>, changes in tectonic uplift rates<sup>3</sup>, climate-induced changes in river incision rate<sup>4,7</sup>, large landslides<sup>8</sup> and glaciation<sup>9</sup>. For example, Niagara Falls formed because of recession of the Laurentide ice-sheet<sup>10</sup>. Thus, waterfalls and steepened channel segments (or knickzones) are used to reconstruct perturbations in environmental forcing, such as climate and tectonism, over millions of years<sup>2,3,11</sup>. However, mechanisms controlling waterfall formation are poorly understood because waterfalls form and evolve over geological timescales, making constraints on waterfall formation rare<sup>6</sup>. Many waterfalls lack a known origin; for example, waterfalls often occur in a series of steps within a knickzone, and it is often difficult to relate each waterfall to a specific external perturbation or lithologic control (Fig. 1).

Here we propose that waterfalls can form autogenically, meaning that waterfalls can form through internal feedbacks between water flow, sediment transport and bedrock incision, in the absence of external perturbations or lithologic controls. If autogenic waterfalls are common, their existence would change our interpretation of tectonic and climatic history recorded in river profiles. Autogenic feedbacks that lead to repeating topographic forms in riverbeds (that is, bedforms) are common, but it is unknown whether similar feedbacks can cause waterfall formation in bedrock. For example, experiments have shown that incising, steep riverbeds rapidly develop repeating, undulating chutes and pools, known as cyclic steps<sup>12–15</sup>, that are self-organized<sup>16,17</sup>. Cyclic steps are similar to waterfalls, but their step height is small relative to their wavelength, and they lack a freefalling jet that defines a waterfall<sup>14,18</sup>. It has been proposed that cyclic steps might develop into waterfalls<sup>12,19</sup>, but this hypothesis has not been tested. Instead, previous experiments have explored waterfall formation due to perturbations in external forcing—such as changes in base level, water discharge or sediment supply<sup>12,16,17,20</sup>—or have used a layered or fractured substrate to promote waterfall formation<sup>21,22</sup>. Moreover, most previous experiments used sediment substrates erodible by clear water alone<sup>12–14,16,17,20</sup>, whereas natural bedrock channels wear by abrasion from particle impacts or plucking. Techniques using scaled concrete or foam produce better quantitative analogues to bedrock<sup>23</sup>, but experiments using these bedrock analogues have yet to explore waterfall formation.

Isolating the relative controls of climate, tectonics, lithology and autogenic dynamics on waterfall formation is challenging because bedrock riverbeds evolve over a thousand years or more and they are subject to autogenic dynamics and allogenic perturbations over varied timescales. To overcome this challenge, we used a physical experiment to test the hypothesis that bedrock waterfalls can form due to autogenic dynamics alone, in the absence of perturbations in external forcing or lithologic controls. The experiment was designed to simplify the natural environment in order to isolate autogenic processes, while maintaining dynamic scaling<sup>24</sup>.

Our experiment used a riverbed 7.3 m long by 30.5 cm wide tilted to a grade of 19.5% (Extended Data Fig. 1). We used a synthetic bedrock of polyurethane foam, which simulates uniform bedrock (for example, Fig. 1) and lacks lithologic heterogeneities known to cause waterfall formation<sup>21,22</sup>. Like natural rock, the foam resists erosion by water alone, and it follows the same erosion scaling law as does natural rock under abrasion by particle impacts<sup>23</sup> (Methods). The bed was planar initially, and we used constant water discharge and supply of unimodal gravel (Methods), making the experiment free of the perturbations in external forcing that are typically thought to cause waterfall formation<sup>2–4</sup>. Hydraulics and sediment transport were scaled on the basis of mountain rivers where waterfalls are common<sup>3</sup>, including Froude-transcritical and turbulent flow (Methods). Erosion-rate scaling suggests that riverbed evolution in our 3.7-h experiment represents about 10<sup>2</sup>–10<sup>5</sup> years of river incision for natural rivers that have flood intermittency and stronger substrates (Methods).

Within the first hour of the experiment, impacts from bed load-transported gravel abraded a channel that was about 8–10 cm wide, and continued incision, in the absence of hillslope processes, led to the formation of a slot canyon (Extended Data Fig. 2). Along the riverbed, decimetre-scale variations in erosion created repeating convex bedrock crests and concave depressions, which grew in amplitude to form cyclic steps, similar to previous experiments<sup>13–15</sup>. The cyclic steps migrated downstream as a result of sediment impacts on the upstream side of bedrock crests (Fig. 2), and hydraulic jumps separated supercritical flow in chutes from subcritical flow in pools (Fig. 3). Unlike previous work with sediment beds, some cyclic steps in our experiment developed into waterfalls starting in the period after 2.1 hours of experiment time and before 3.1 hours. Waterfalls formed as deeper pools trapped sediment that armoured their bases against erosion, whereas vertical incision continued in the next pool downstream, causing the chute between the armoured pool and its downstream neighbour to steepen (Fig. 2; Extended Data Figs. 3 and 4; Extended Data Table 1). The combination of deposition in the upstream pool and flattening of the pool's downstream lip created a smoothed reach over which water accelerated and detached at the steepened chute, forming a waterfall with a fully ventilated jet and plunge pool (Supplementary Videos 1 and 2). Two waterfalls formed with peak heights of 35 cm and 38 cm (about 3.5-fold and 6-fold the flow depth at the waterfall brink) (Extended Data Table 1). The escarpments had maximum slopes of 45° and 49°, similar to natural waterfalls in massive rock<sup>3</sup> (Fig. 1 and Extended Data Figs. 5 and 6). In contrast to the cyclic steps, individual waterfalls showed negligible migration. Waterfalls persisted for about 20 min (representing about 10<sup>1</sup>–10<sup>4</sup> years in natural rivers; see Methods) before erosion at the

<sup>1</sup>Division of Geological and Planetary Sciences, California Institute of Technology, Pasadena, CA, USA. <sup>2</sup>GFZ German Research Centre for Geosciences, Telegrafenberg, Potsdam, Germany. <sup>3</sup>Present address: Department of Geological Sciences and Engineering, University of Nevada Reno, Reno, NV, USA. \*e-mail: [jscheingross@unr.edu](mailto:jscheingross@unr.edu)



**Fig. 1 | Repeating waterfalls formed in relatively homogeneous rock.** **a**, Kohala Peninsula (Hawaii, USA). **b**, Eaton Canyon (photo credit: Roman DiBiase). **c**, Fox Creek (San Gabriel Mountains, USA). **d**, Dry Meadow

(photo credit: Devon Santy). **e**, Dinkey Creek (Sierra Nevada, USA) (photo credit: Darin McQuoid). Waterfall slopes range from about 45° to 90°.

waterfall brink reduced the waterfall height causing flow reattachment to the riverbed (Extended Data Fig. 3). As waterfalls were destroyed, the plunge-pool lip upstream of the waterfall steepened, leading, in one case, to a new proto-waterfall and plunge pool (Fig. 2g). Our experiment had reach-averaged erosion rates approximately 2-fold higher than predicted for planar beds (Methods).

Autogenic waterfalls formed in our experiment as a result of feedbacks between water flow, sediment transport and bedrock topography in the absence of rock fractures, bedding or external perturbations to base level, water discharge or sediment supply. Autogenic waterfall formation is tied to the nonlinear role of sediment in bedrock-bed stability, dynamics that may have been absent in experiments with sediment beds erodible by water alone<sup>12,16,17,20</sup>. In bedrock, zones of frequent, high-energy impacts erode rapidly, such as in shallow pools; however, spatial convergences in sediment flux, such as in deep pools, cause deposition and armouring of the riverbed. Waterfalls form when deposition in an upstream pool prevents erosion, while erosion downstream increases the vertical drop between adjacent pools. Waterfall jets can erode deep plunge pools, when unarmoured, and outpace incision at the waterfall brink<sup>19</sup>, thereby developing waterfall relief. However, drag in deeper pools reduces the particle impact energy, slowing pool incision<sup>19</sup>, and continued waterfall brink erosion eventually destroys the step (Fig. 2; Extended Data Figs. 3 and 4).

Unlike models of waterfalls migrating upstream<sup>10</sup>, in our experiment waterfalls were stationary because the freefalling jet focused impacts on the plunge-pool floor rather than walls<sup>19</sup> (Supplementary Videos 1 and 2). Instead, our findings are consistent with escarpment retreat via a series of vertically eroding waterfalls, in which waterfalls are repeatedly created and destroyed<sup>5,8,19</sup>. In this model, flow acceleration towards the

brink of an existing waterfall<sup>2,25</sup> (Fig. 2e) leads to the generation of cyclic steps upstream of the waterfall<sup>12,15,16</sup>, which then grow via vertical plunge-pool erosion to form new waterfalls (Fig. 2f, g). Although there exists limited evidence of waterfall lifetimes, our scaled experiment suggests that individual autogenic waterfalls may persist for up to 10<sup>4</sup> years, and continual creation of waterfalls would result in longer-lived escarpment retreat.

Our experiment suggests that self-formed waterfalls can form from a bedrock riverbed undergoing erosion by abrasion, and near Froude-critical flow (Froude number near unity). Near-Froude-critical flow conditions are common to streams with slopes exceeding a grade of 1% (refs<sup>12,26</sup>), which dominate drainage networks in mountainous terrain, suggesting that autogenic waterfalls could be widespread. However, more work is needed to identify the necessary conditions for self-formed waterfalls and fingerprint their attributes. Waterfalls in our experiment had drop heights of 3 to 6 times the flow depth, but this is unlikely to be diagnostic; the relative height probably depends on water discharge and sediment supply, which need to be systematically explored. Our experiment indicates that autogenic waterfalls should occur as a series of steps, with initial spacing set by the cyclic-step instability<sup>18</sup>. Waterfalls in series are common (Fig. 1), and it is often difficult to link a specific external perturbation or rock heterogeneity to each individual waterfall, consistent with an autogenic interpretation. Conversely, the presence of a single, isolated waterfall (for example, Niagara Falls) is inconsistent with autogenic formation, which requires cyclic steps as precursors to waterfalls.

In our experiment, the initial bed slope was imposed. In natural landscapes, steep riverbed slopes, capable of supercritical flow and autogenic waterfalls, might develop under steady external forcing or due to perturbations in forcing. For example, landscape evolution models under steady

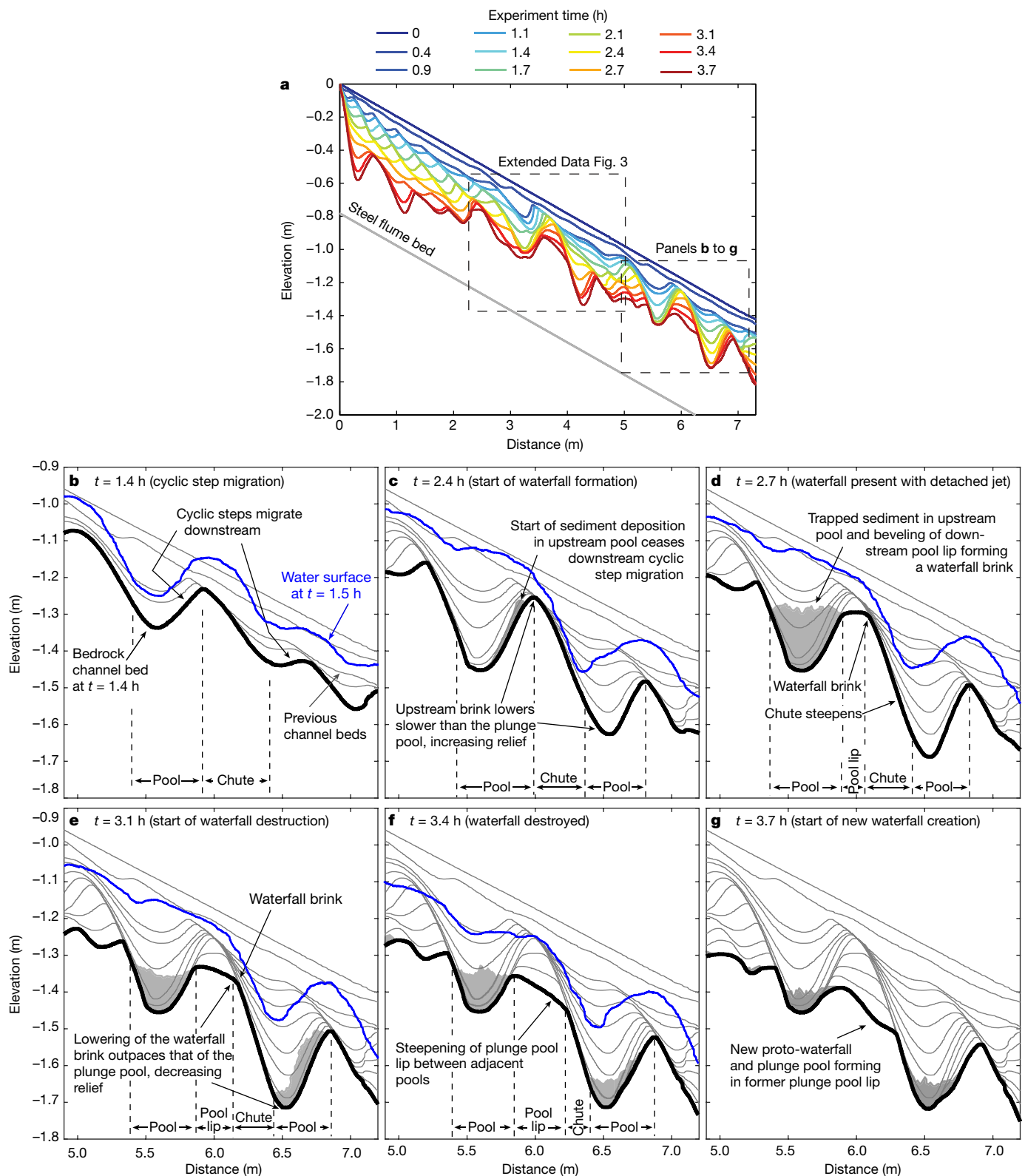


**Fig. 2 | Bedrock channel evolution.** **a**, Laser scan of bedrock profile evolution. **b–g**, Detailed bedrock and water surface topographic profiles for the given times; grey shading shows sediment armouring. Light-grey profiles are spaced at approximately 0.3-h intervals. Water surface profiles

were taken about 0.1 h later than bedrock profiles; no water surface profile is available for **g**. Raw data are provided in the Supplementary Information.

forcing evolve towards a topographic steady state with smooth, concave river profiles<sup>2</sup>. Knickzones and waterfalls emerge in these models only as a result of imposed lithologic variability or perturbations in external forcing<sup>2</sup>. Our experiment suggests, by contrast, that steeper riverbed reaches in steady-state landscapes can develop waterfalls and intervening flatter

reaches in the absence of external perturbations—dynamics absent in existing models<sup>2</sup>, including those used to invert topography for uplift history<sup>11</sup>. A potential example is the Central Sierra Madre Block of the San Gabriel Mountains, California, USA, which has been proposed to be a topographic steady-state landscape<sup>27</sup> because it has had similar erosion

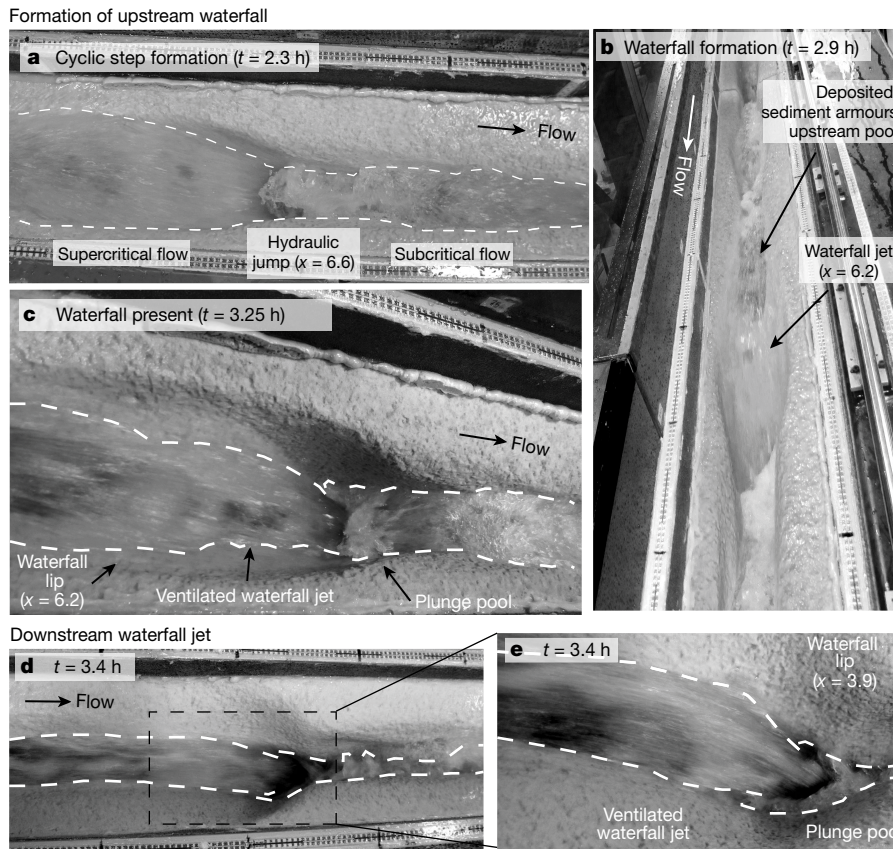


**Fig. 3 | Waterfall formation.** a–c, Upstream waterfall formation. d and e show details of the downstream waterfall jet. We note that the surface on which the flume rests is tilted 19.5% with respect to the horizontal.

rates across decadal-to-million year timescales<sup>27,28</sup>, and uniform granitic rocks are not thought to impact landscape evolution<sup>28</sup>. Rivers within this region (Rubio Canyon and Eaton Canyon; Fig. 1b) have many waterfalls in series that lack association with lithologic boundaries (Extended Data Fig. 6), consistent with an autogenic origin.

Steep riverbeds also form through perturbations in external forcing, such that self-formed waterfalls might develop in concert with externally forced knickzones. For example, previous studies have shown that a single perturbation in external forcing can cause the formation of multiple waterfalls<sup>3,5,8</sup>. In addition, cyclic steps and proto-waterfalls are common upstream of waterfalls because supercritical flow develops as water accelerates towards the waterfall brink<sup>25</sup>. In the Big Tujunga Creek catchment, California, USA, many tributaries, such as Fox Creek (Fig. 1c), have a knickzone that has been linked to an increase in uplift rate<sup>3</sup>. Each knickzone is composed of numerous waterfalls that lack known origins, are consistent with autogenic formation, and have probably changed erosion rates of the broader knickzone in a manner that is inconsistent with fluvial incision models<sup>3</sup>. Bridalveil Creek in Yosemite Valley, California, USA, provides another example, in which the Bridalveil Falls formed along the steep glacially carved valley walls following deglaciation<sup>9</sup>. Despite the allogenic origin of Bridalveil Falls, many additional waterfalls exist upstream of the main falls that are consistent with an autogenic origin (Extended Data Fig. 5c). The upstream waterfalls developed in massive granitic rock, lack an association with jointing (Extended Data Fig. 5b), are unaffected by the base level owing to being upstream of the hanging valley, and are unlikely to have a glacial origin given that they have been ice-free for 800,000 years<sup>9</sup>. Individual waterfalls along Bridalveil Creek coalesce in a regional knickzone about 3 km long similar to those commonly attributed to perturbations in external forcing<sup>2,3,11</sup> (Extended Data Fig. 5c).

The generation of self-formed waterfalls illustrates the complex evolution of incising bedrock channels in response to constant forcing. The emergence of waterfalls is important for landscape evolution because

a series of waterfalls can change river incision rates<sup>19</sup> and river-profile concavity over kilometre scales<sup>3</sup>. Thus, autogenic waterfalls can affect bedrock erosion, sediment production and hillslope gradients that drive landsliding<sup>1</sup>, potentially driving oscillations in sediment flux<sup>29</sup>. The existence of knickzones and waterfalls is often used to define landscape topographic disequilibrium with respect to external forcing<sup>2</sup>. By contrast, our experiment suggests that waterfalls may be able to emerge in landscapes with uniform lithology undergoing steady external forcing, which could lead to erroneous identification of changes in climate and tectonics from channel profile inversion. Autogenic waterfalls that emerge in response to externally forced river steepening may change the rates that allogenic perturbations propagate through river networks, further obscuring climate and tectonic signals.

### Online content

Any methods, additional references, Nature Research reporting summaries, source data, statements of data availability and associated accession codes are available at <https://doi.org/10.1038/s41586-019-0991-z>.

Received: 23 February 2018; Accepted: 7 January 2019;  
Published online 13 March 2019.

- Weissel, J. K. & Seidl, M. A. in *Rivers Over Rock: Fluvial Processes In Bedrock Channels* (eds Tinkler, K. & Wohl, E.) 189–206 (Geophysical Monograph, AGU, Washington DC, 1998).
- Whipple, K. X., DiBiase, R. A. & Crosby, B. T. in *Treatise on Geomorphology* Vol. 9 (eds Shroder, J. Jr & Wohl, E. E.) Ch. 9.28, 550–573 (Elsevier, London, 2013).
- DiBiase, R. A., Whipple, K. X., Lamb, M. P. & Heimsath, A. M. The role of waterfalls and knickzones in controlling the style and pace of landscape adjustment in the western San Gabriel Mountains, California. *Geol. Soc. Am. Bull.* **127**, 539–559 (2015).
- Crosby, B. T. & Whipple, K. X. Knickpoint initiation and distribution within fluvial networks: 236 waterfalls in the Waipaoa River, North Island, New Zealand. *Geomorphology* **82**, 16–38 (2006).
- Howard, A. D., Dietrich, W. E. & Seidl, M. A. Modeling fluvial erosion on regional to continental scales. *J. Geophys. Res. Solid Earth* **99**, 13971–13986 (1994).

6. Yanites, B. J., Tucker, G. E., Mueller, K. J. & Chen, Y. G. How rivers react to large earthquakes: evidence from central Taiwan. *Geology* **38**, 639–642 (2010).
  7. Malatesta, L. C. & Lamb, M. P. Formation of waterfalls by intermittent burial of active faults. *Geol. Soc. Am. Bull.* **130**, 522–536 (2018).
  8. Lamb, M. P., Howard, A. D., Dietrich, W. E. & Perron, J. T. Formation of amphitheater-headed valleys by waterfall erosion after large-scale slumping on Hawai'i. *Geol. Soc. Am. Bull.* **119**, 805–822 (2007).
  9. Matthes, F. E. *Geologic History of the Yosemite Valley* (USGS Professional Paper 160, United States Government Printing Office, Washington DC, 1930).
  10. Gilbert, G. K. The history of the Niagara River, extracted from the sixth annual report to the commissioners of the state reservation at Niagara, Albany, NY. <https://babel.hathitrust.org/cgi/pt?id=mdp.39015059496375;view=1up;seq=1> (1890).
  11. Roberts, G. G., White, N. J. & Shaw, B. An uplift history of Crete, Greece, from inverse modeling of longitudinal river profiles. *Geomorphology* **198**, 177–188 (2013).
  12. Baynes, E. R. C., Lague, D. & Kermarrec, J. Supercritical river terraces generated by hydraulic and geomorphic interactions. *Geology* **46**, 499–502 (2018).
  13. Brooks, P. C. *Experimental Study of Erosional Cyclic Steps*. Masters thesis, Univ. Minnesota (2001).
  14. Taki, K. & Parker, G. Transportational cyclic steps created by flow over an erodible bed. Part 1. Experiments. *J. Hydraul. Res.* **43**, 488–501 (2005).
  15. Yokokawa, M., Kotera, A. & Kyogoku, A. in *Advances in River Sediment Research* (eds S. Fukuoka et al.) 629–333 (CRC Press, Leiden, 2013).
  16. Grimaud, J. L., Paola, C. & Voller, V. Experimental migration of knickpoints: influence of style of base-level fall and bed lithology. *Earth Surf. Dyn.* **4**, 11–23 (2016).
  17. Baynes, E. R. C. et al. River self-organisation inhibits discharge control on waterfall migration. *Sci. Rep.* **8**, 2444 (2018).
  18. Izumi, N., Yokokawa, M. & Parker, G. Incisional cyclic steps of permanent form in mixed bedrock-alluvial rivers. *J. Geophys. Res. Earth Surf.* **122**, 130–152 (2017).
  19. Scheingross, J. S. & Lamb, M. P. A mechanistic model of plunge pool erosion into bedrock. *J. Geophys. Res. Earth Surf.* **122**, 2079–2104 (2017).
  20. Gardner, T. W. Experimental study of knickpoint and longitudinal profile evolution in cohesive, homogenous material. *Geol. Soc. Am. Bull.* **94**, 664–672 (1983).
  21. Holland, W. N. & Pickup, G. Flume study of knickpoint development in stratified sediment. *Geol. Soc. Am. Bull.* **87**, 76–82 (1976).
  22. Lamb, M. P. & Dietrich, W. E. The persistence of waterfalls in fractured rock. *Geol. Soc. Am. Bull.* **121**, 1123–1134 (2009).
  23. Lamb, M. P., Finnegan, N. J., Scheingross, J. S. & Sklar, L. S. New insights into the mechanics of fluvial bedrock erosion through flume experiments and theory. *Geomorphology* **244**, 33–55 (2015).
  24. Paola, C., Straub, K., Mohrig, D. & Reinhardt, L. The “unreasonable effectiveness” of stratigraphic and geomorphic experiments. *Earth Sci. Rev.* **97**, 1–43 (2009).
  25. Haviv, I. et al. Amplified erosion above waterfalls and oversteepened bedrock reaches. *J. Geophys. Res. Earth Surf.* **111**, F04004 (2006).
  26. Palucis, M. C. & Lamb, M. P. What controls channel form in steep mountain streams? *Geophys. Res. Lett.* **44**, 7245–7255 (2017).
  27. Lave, J. & Burbank, D. Denudation processes and rates in the Transverse Ranges, southern California: erosional response of a transitional landscape to external and anthropogenic forcing. *J. Geophys. Res. Earth Surf.* **109**, F01006 (2004).
  28. DiBiase, R. A., Whipple, K. X., Heimsath, A. M. & Ouimet, W. B. Landscape form and millennial erosion rates in the San Gabriel Mountains, CA. *Earth Planet. Sci. Lett.* **289**, 134–144 (2010).
  29. Hasbargen, L. E. & Paola, C. Landscape instability in an experimental drainage basin. *Geology* **28**, 1067–1070 (2000).
- Acknowledgements** We thank J. Preimesberger for assistance with preliminary experiments, R. DiBiase, W. Dietrich, N. Izumi, G. Parker, J. Prancevic, J. Turowski and M. Yokokawa for discussion, and A. Wickert for a review. We acknowledge funding from the National Science Foundation (grant EAR-1147381 to M.P.L. and a Graduate Research Fellowship to J.S.S.), NASA (grant 12PGG120107 to M.P.L.), and the Alexander von Humboldt Foundation (postdoctoral fellowship to J.S.S.). This work includes data services provided by the OpenTopography Facility with support from the National Science Foundation under NSF Award Numbers 1557484, 1557319 and 1557330, and EAR-1043051.
- Reviewer information** *Nature* thanks Andrew Wickert and the other anonymous reviewer(s) for their contribution to the peer review of this work.
- Author contributions** J.S.S. and M.P.L. designed the study and wrote the manuscript with input from B.M.F. J.S.S. and B.M.F. performed the experiment with input from M.P.L.
- Competing interests** The authors declare no competing interests.
- Additional information**  
**Extended data** is available for this paper at <https://doi.org/10.1038/s41586-019-0991-z>.  
**Supplementary information** is available for this paper at <https://doi.org/10.1038/s41586-019-0991-z>.  
**Reprints and permissions information** is available at <http://www.nature.com/reprints>.  
**Correspondence and requests for materials** should be addressed to J.S.S.  
**Publisher's note:** Springer Nature remains neutral with regard to jurisdictional claims in published maps and institutional affiliations.

© The Author(s), under exclusive licence to Springer Nature Limited 2019

## METHODS

Water discharge, sediment supply, and grain size were selected so that the experiment initially had supercritical flow, while keeping sediment supply well below transport capacity to allow bedrock exposure. We fed unimodal, siliciclastic sediment at a constant rate of  $0.5 \pm 0.02 \text{ kg s}^{-1}$  (mean  $\pm$  standard deviation), with a median grain diameter of  $D = 2.4 \text{ cm}$  to maximize erosion via high kinetic impact energy, and to ensure large particle Reynolds numbers ( $>5.0 \times 10^4$ ) typical of mountain streams. Water discharge was held constant at  $Q_w = 14.2$  litres per second, the initial reach-averaged Shields stress ( $\tau^* \approx 0.11$ ) was in excess of the threshold of motion, and the gravel moved as bedload. Flow was fully turbulent (Reynolds numbers of  $10^4$  to  $10^5$ ). The initially high Froude number flow ( $Fr \approx 4.5$  at  $t = 0$ ) reduced to  $Fr \approx 2$  by  $t = 0.4 \text{ h}$ , and flow was trans-critical after  $t \approx 1.7 \text{ h}$  due to cyclic step development. The base level was fixed 44 cm below the end of our experimental test section (Extended Data Fig. 1), allowing the channel upstream to erode freely over the duration of the experiment. Importantly, the cyclic steps and waterfalls emerged far upstream of the downstream boundary and were not influenced by the base level.

As a bedrock simulant, we installed an initially planar 76-cm-thick bed of low-tensile strength ( $\sigma_T = 0.32 \text{ MPa}$ ) polyurethane foam (Extended Data Fig. 1). This homogeneous foam quantitatively simulates massive rock in which waterfalls often form (Fig. 1), and lacks the fractures and bedding that are known to force waterfall formation<sup>1,21,22</sup>. The foam follows the same tensile-strength versus erosion rate scaling observed in natural rock and concrete, allowing scaling of erosion rates between the laboratory and natural streams<sup>23,30</sup>, and increased laboratory erosion rates due to the low-tensile strength foam. Eroded foam particles entered the wash load and did not contribute to channel erosion. Prior to the start of the experiment, we ran 20 h of clear-water discharge with zero sediment supply (under otherwise identical conditions to the main experiment), observing no detectable erosion of the foam. By contrast, measurable erosion occurred within minutes of initiating sediment feed, indicating that foam erosion occurred exclusively due to abrasion from particle impacts.

The water-surface elevation was measured along the channel thalweg at horizontal spacing of 1 mm using a sub-millimetre vertical resolution laser scanner that illuminated the aerated water surface. The experiment was paused every 3 min to 30 min to measure bedrock topography with the same laser scanner at resolutions of 1 mm in the along-stream direction and 2–10 mm in the cross-stream direction. Where sediment was deposited, we first scanned the bed with the sediment in place, then removed sediment by hand and scanned the bedrock surface, and finally replaced the sediment before resuming the experiment. The waterfall drop

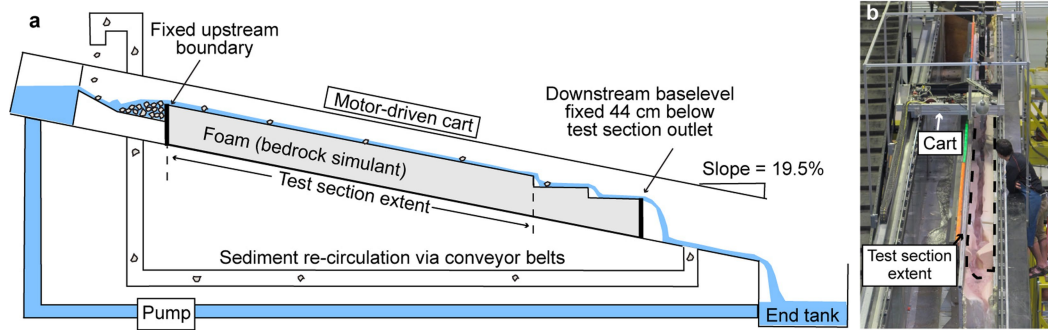
height was measured as the vertical distance between the point of jet detachment from the bedrock surface and the minimum elevation of the downstream plunge-pool bedrock floor. Reach-averaged erosion rates were calculated by differencing successive topographic scans and taking spatial averages. These rates were compared with theoretical predictions for a planar bed using a bedrock erosion model which accounts for erosion from bedload and suspended sediment<sup>31</sup>, with all values set to those in the experiment, and calibrated for the foam substrate<sup>30</sup>.

To compare the timescale of erosion between the experiment and natural channels, we propose that the characteristic timescale to form autogenic waterfalls,  $T$ , scales with the time to vertically incise, at rate  $E$ , a distance equivalent to one channel depth,  $h$ , that is,  $T_{\text{laboratory}} \propto h_{\text{laboratory}}/E_{\text{laboratory}}$  and  $T_{\text{field}} \propto h_{\text{field}}/E_{\text{field}}$ , where the subscripts ‘laboratory’ and ‘field’ refer to the laboratory and field conditions, respectively. We solved for  $T$  using average values from our experiment ( $h_{\text{laboratory}} = 130 \text{ mm}$  and  $E_{\text{laboratory}} = 100 \text{ mm h}^{-1}$ ) and a range of values appropriate for mountain rivers where waterfalls are common ( $1 \text{ m} < h_{\text{field}} < 6 \text{ m}$  and  $10^{-2} \text{ mm yr}^{-1} < E_{\text{field}} < 10^1 \text{ mm yr}^{-1}$ )<sup>32,33</sup>.  $T_{\text{field}}/T_{\text{laboratory}}$  ranges from  $10^5$  to  $10^8$ ; the ratio is large mostly because the foam has low tensile strength and because of the lack of flood intermittency in the laboratory.

## Data availability

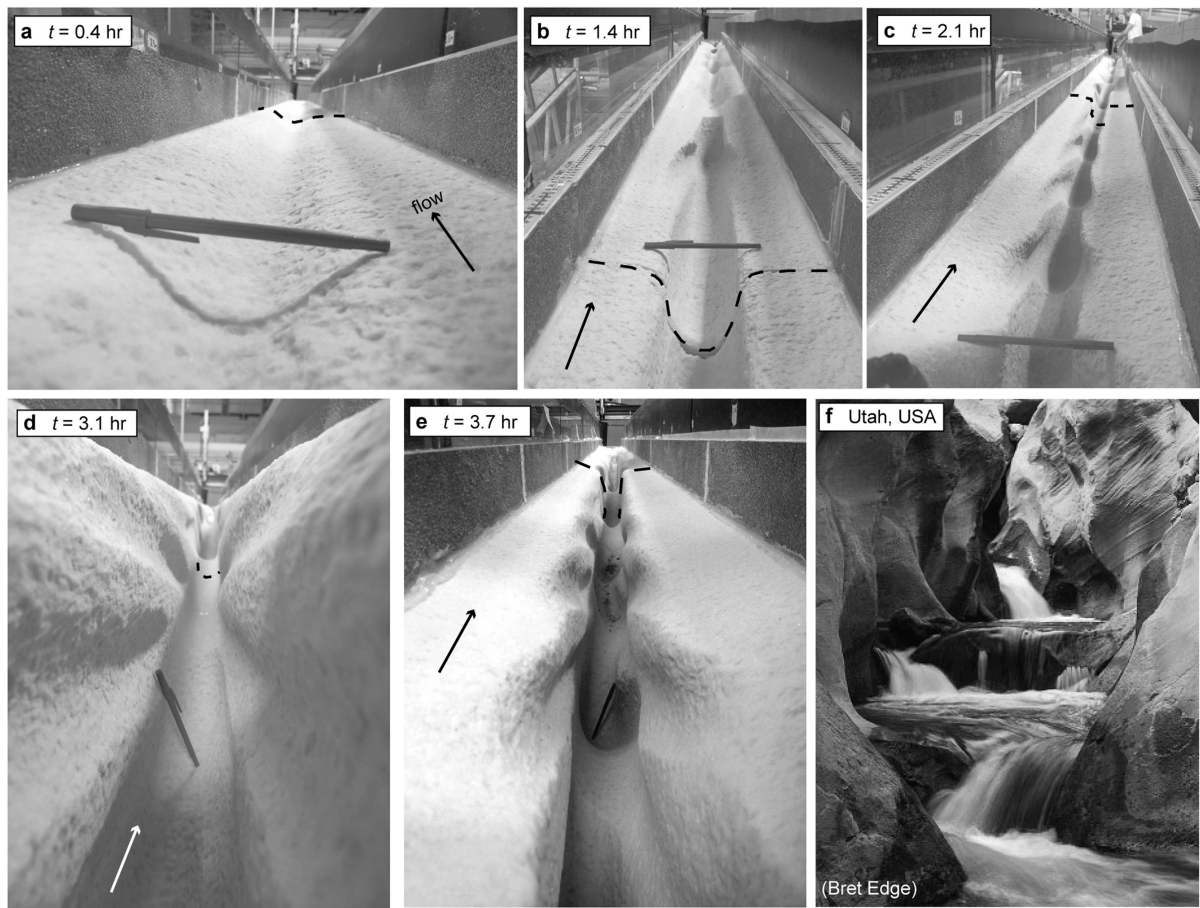
All topographic and water surface profiles are available in the Supplementary Information.

30. Scheingross, J. S., Brun, F., Lo, D. Y., Omerdin, K. & Lamb, M. P. Experimental evidence for fluvial bedrock incision by suspended and bedload sediment. *Geology* **42**, 523–526 (2014).
31. Lamb, M. P., Dietrich, W. E. & Sklar, L. S. A model for fluvial bedrock incision by impacting suspended and bed load sediment. *J. Geophys. Res. Earth Surf.* **113**, F03025 (2008).
32. Finnegan, N. J., Roe, G., Montgomery, D. R. & Hallet, B. Controls on the channel width of rivers: implications for modeling fluvial incision of bedrock. *Geology* **33**, 229–232 (2005).
33. Portenga, E. W. & Bierman, P. R. Understanding Earth’s eroding surface with <sup>10</sup>Be. *GSA Today* **21**, <https://doi.org/10.1130/G1111A.1> (2011).
34. Yerkes, R. F. & Campbell, R. H. *Preliminary Geologic Map of the Los Angeles 30' x 60' Quadrangle, Southern California, Washington DC*. Open-File Report 2005–1019 <https://pubs.usgs.gov/of/2005/1019/> (US Geological Survey, 2005).
35. Stock, G. *Yosemite, CA: El Portal, Mariposa Grove, Yosemite Canyon & Tuolumne Meadows*. <https://doi.org/10.5069/G9GQ6VP3> (National Center for Airborne Laser Mapping (NCALM), OpenTopography, 2006).



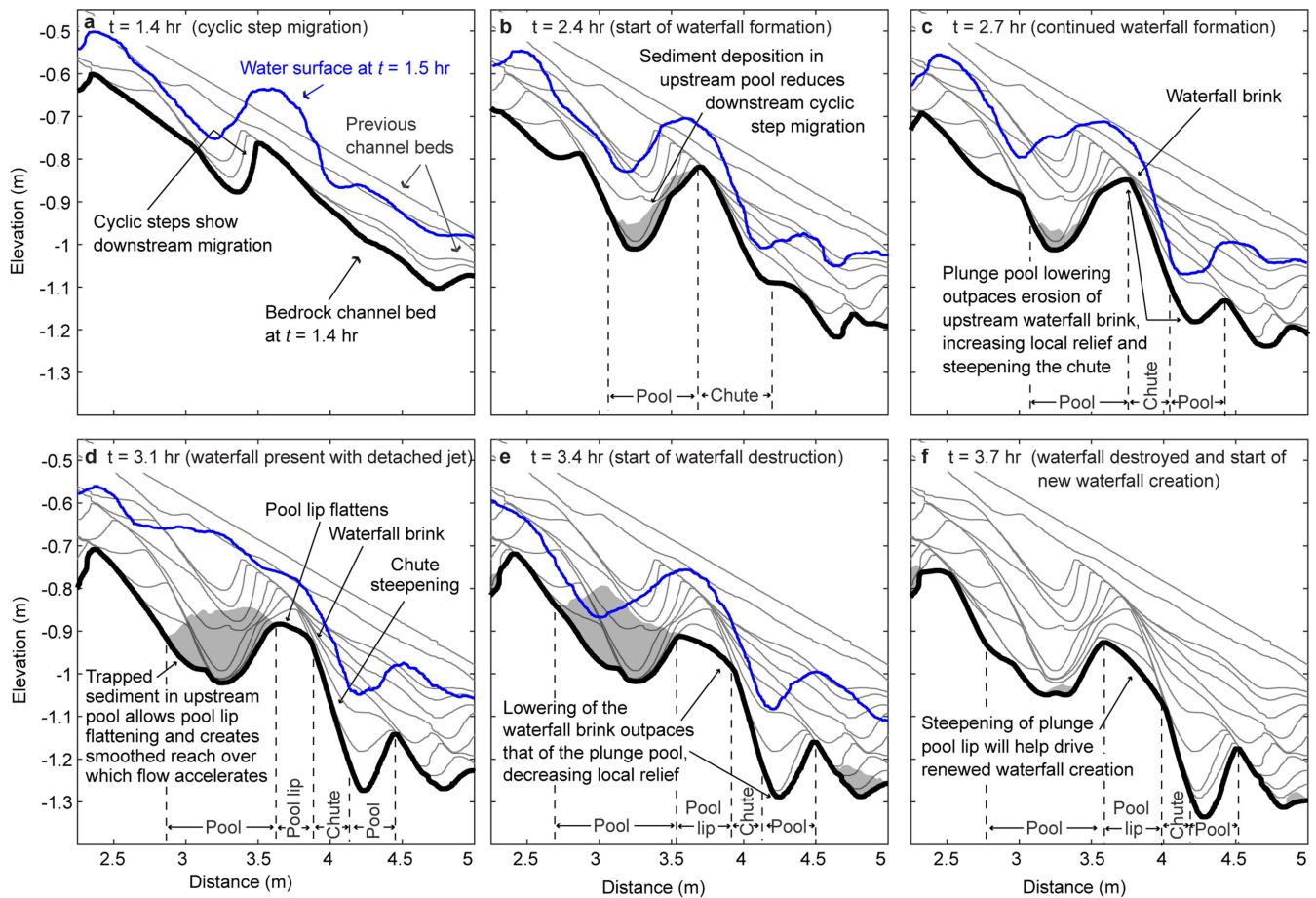
**Extended Data Fig. 1 | Experimental set-up.** **a**, Schematic of experimental set-up at  $t = 0$  h. Precut steps visible downstream of the test section extent eroded rapidly to the fixed base level and did not influence

the experiment or the development of cyclic steps (which developed throughout the test section). **b**, Photograph (taken by B.M.F.) of set-up after completion of the experiment.



**Extended Data Fig. 2 | Experiment photographs showing canyon incision.** a–e, Progressive incision and canyon formation with time. The dashed line highlights the  $x = 2.3$  m cross-section; the arrow points downstream (a 15-cm-long pen is shown to give the scale). Photographs

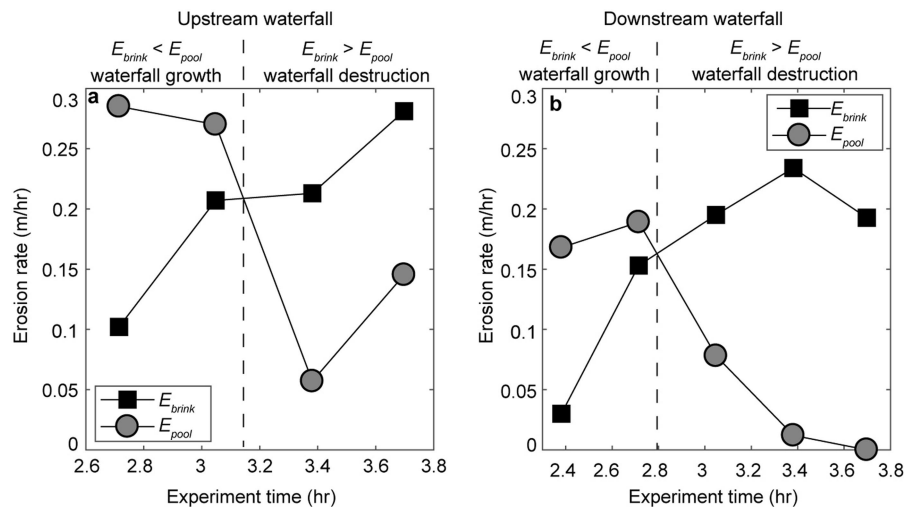
were taken (by authors) after removal of deposited sediment while the experiment was paused. f, Field example of a canyon with similar morphology to our experiment from Pleasant Creek, Capitol Reef National Park, Utah, USA (photo credit: Bret Edge).



### Extended Data Fig. 3 | Detail view of bedrock channel evolution.

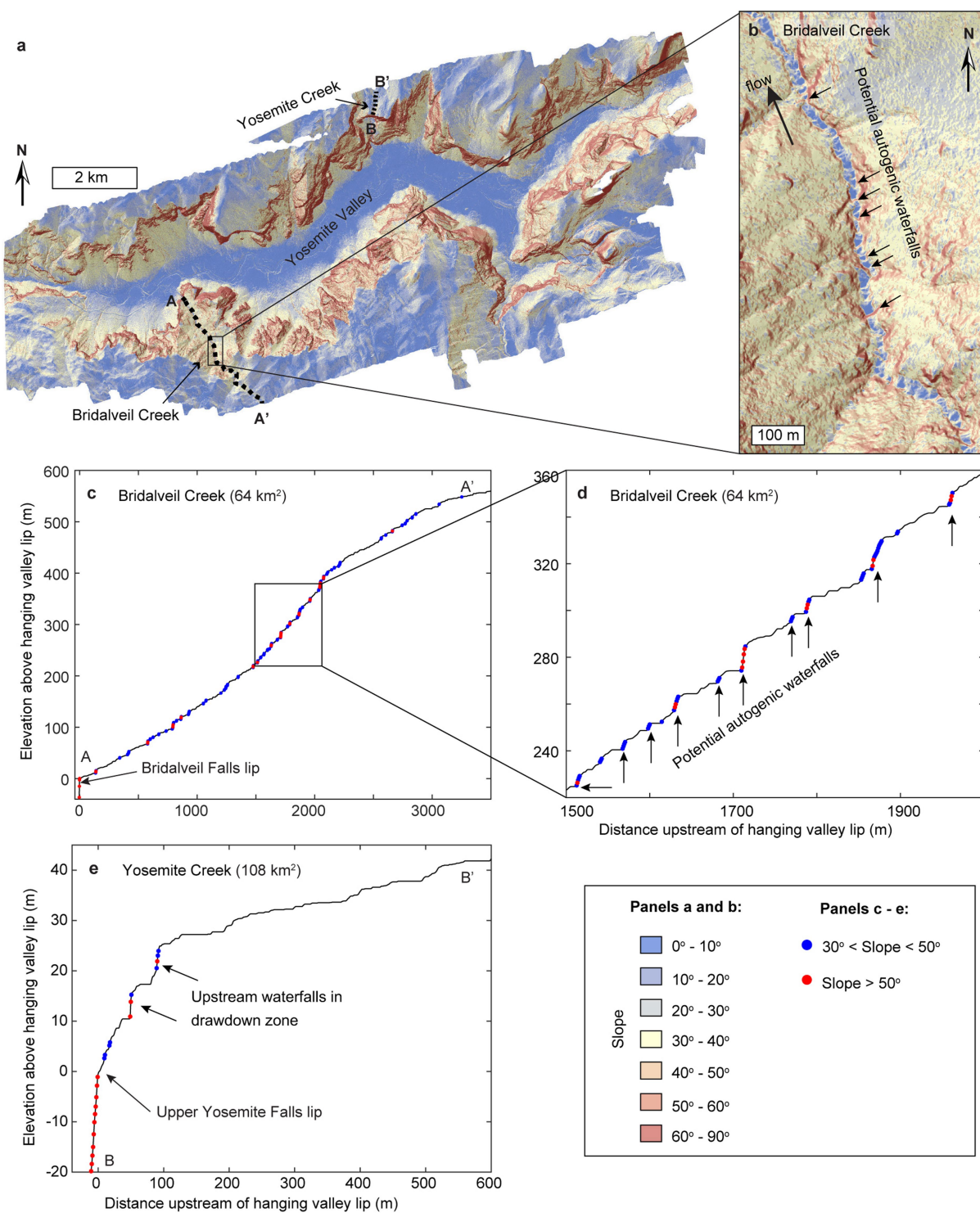
**a–f**, Time series of bedrock channel (black) and water surface (blue) profiles showing waterfall plunge-pool formation at  $x \approx 4$  m. Grey lines show previous bedrock surfaces spaced at about 0.3-h intervals and

correspond to times shown in Fig. 2a; grey shading denotes areas of deposited sediment. We note that water surface profiles correspond to times about 0.1 h later than bedrock profiles and no water surface profile is available for **f**. Raw data are provided in Supplementary Data 1.



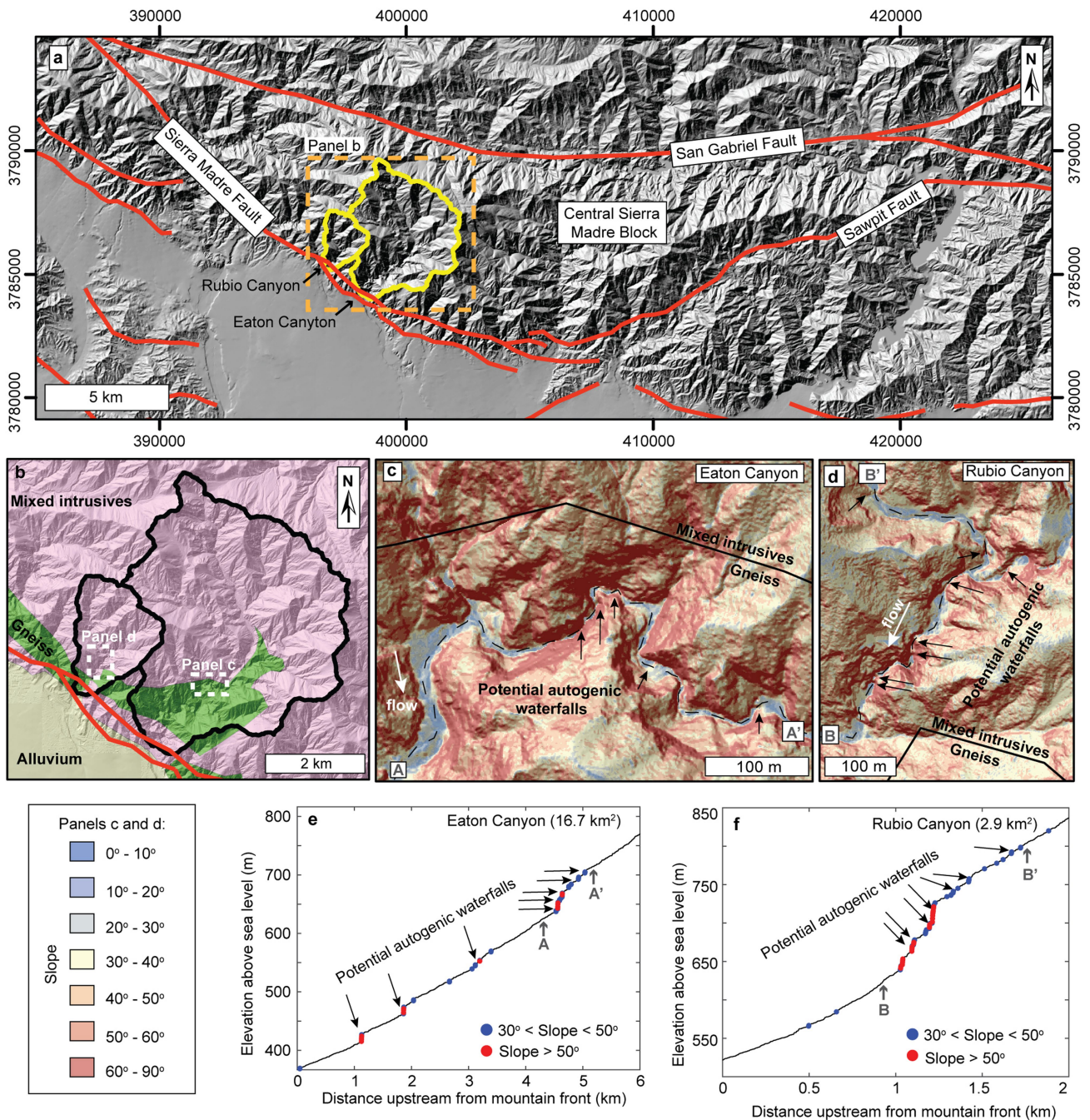
**Extended Data Fig. 4 | Relative vertical erosion rates at the waterfall brink and the waterfall plunge-pool floor. a**, Erosion rate versus time for the upstream waterfall centred at  $x = 4.3$ . **b**, Erosion rate versus time for the downstream waterfall centred at  $x = 6.5$ . During periods of waterfall formation ( $2.4 \text{ h} < t < 3.1 \text{ h}$  and  $2.1 \text{ h} < t < 2.8 \text{ h}$  for the upstream and

downstream waterfall, respectively) erosion at the pool floor ( $E_{floor}$ ) outpaced that at the brink ( $E_{brink}$ ), causing an increase in waterfall height. As waterfall plunge pools deepened, their erosion rates slowed below that of the upstream brink, thereby decreasing waterfall height and destroying the original waterfall.



**Extended Data Fig. 5 | Field examples of putative autogenic waterfalls formed in concert with externally forced riverbed steepening.** **a**, Lidar shaded relief map of Yosemite Valley, California, USA. **b**, Detailed view of potentially autogenic waterfalls upstream of Bridalveil Falls (data distributed via OpenTopography<sup>35</sup>). We note that waterfalls do not align

with macroscale jointing or fractures visible in the lidar. **c–e**, Lidar-extracted long profiles above Bridalveil (**c**, **d**) and Upper Yosemite Falls (**e**). Coloured dots show channel slopes above 30° calculated across a 3-pixel moving window (horizontal length scale of about 3 m). Waterfalls frequently occur at slopes less than 50°, similar to our experiment.



**Extended Data Fig. 6 | Field examples of putative autogenic waterfalls formed in steady-state landscapes.** **a**, Shaded relief map of the Central Sierra Madre Block of the San Gabriel Mountains, California, USA, showing locations of the Eaton and Rubio canyons. **b**, Simplified geological map of Rubio and Eaton canyons after ref. <sup>34</sup>, mixed intrusive rocks are dominated by Cretaceous and Triassic granitoids. **c**, **d**, Detailed lidar

shaded relief maps showing potentially autogenic waterfalls in the Eaton and Rubio canyons (data courtesy of the National Center for Airborne Laser Mapping (NCALM) and available in Supplementary Data 2). **e**, **f**, Lidar-extracted long profile for Eaton and Rubio canyons with coloured dots showing channel slopes above 30° calculated across a 3-pixel moving window (horizontal length scale of about 3 m).

**Extended Data Table 1 | Elevation and erosion rates of waterfalls**

Experiment Time (hr)	$Z_{brink}$ (m)	$Z_{pool}$ (m)	$Z_{brink} - Z_{pool}$ (m)	$E_{brink}$ (m/hr)	$E_{pool}$ (m/hr)	$E_{brink} / E_{pool}$
Upstream waterfall centered at $x = 4.2$						
2.38	-0.82	-1.09	0.27			
2.71	-0.85	-1.18	0.33	0.10	0.29	0.36
3.05	-0.92	-1.27	0.35	0.21	0.27	0.77
3.38	-0.99	-1.29	0.30	0.21	0.06	3.74
3.70	-1.08	-1.34	0.26	0.28	0.15	1.93
Downstream waterfall centered at $x = 6.5$						
2.05	-1.24	-1.57	0.32			
2.38	-1.25	-1.62	0.37	0.03	0.17	0.18
2.71	-1.31	-1.69	0.38	0.15	0.19	0.81
3.05	-1.37	-1.71	0.34	0.20	0.08	2.50
3.38	-1.45	-1.72	0.27	0.23	0.01	19.50
3.70	-1.51	-1.72	0.21	0.19	0.00	

$Z_{brink}$  and  $Z_{pool}$  are the elevations of the plunge pool upstream brink and floor, respectively.  $E_{brink}$  and  $E_{pool}$  are the vertical lowering rate of the plunge pool upstream brink and floor, respectively.